High resolution x-ray diffraction study of the substrate temperature and thickness dependent microstructure of reactively sputtered epitaxial ZnO films

High resolution x-ray diffraction study of the substrate temperature and thickness dependent microstructure of reactively sputtered epitaxial ZnO films

D. Singh[1,#,*], R. Kumar[2], T. Ganguli[3] and S. S. Major[4]

[1]Centre for Research in Nanotechnology and Sciences, Indian Institute of Technology Bombay, Mumbai-400076, India

[2]Semiconductor Materials Laboratory, Materials Science Section, Raja Ramanna Centre for Advanced Technology, Indore-452013, India

[3]Materials Research Laboratory, Synchrotron Utilization Section, Raja Ramanna Centre for Advanced Technology, Indore-452013, India

[4]Department of Physics, Indian Institute of Technology Bombay, Mumbai-400076, India

[#]Present Address: Division of Physical Engineering and Science, King Abdullah University of Science and Technology, Thuwal-23955-6900, KSA.

*Corresponding author. E-mail: dsingh.iitb@gmail.com

Tel.: +966 (02) 808-869; Fax: +91-22-25767552

Abstract

Epitaxial ZnO films were grown on c-sapphire by reactive sputtering of zinc target in Ar-O_2 mixture. High resolution X-ray diffraction measurements were carried out to obtain lateral and vertical coherence lengths, crystallite tilt and twist, micro-strain and densities of screw and edge dislocations in epilayers of different thickness (25 - 200 nm) and those grown at different temperatures (100 - 500 °C). ϕ-scans indicate epitaxial growth in all the cases, although epilayers grown at lower substrate temperatures (100 °C and 200 °C) and those of smaller thickness (25 nm and 50 nm) display inferior microstructural parameters. This is attributed to the dominant presence

of initially grown strained 2D layer and subsequent transition to an energetically favorable mode. With increase in substrate temperature, the transition shifts to lower thickness and growth takes place through the formation of 2D platelets with intermediate strain, over which 3D islands grow. Consequently, 100 nm thick epilayers grown at 300 °C display the best microstructural parameters (micro-strain ~1.2 x 10^{-3}, screw and edge dislocation densities ~1.5 x 10^{10} cm^{-2} and ~2.3 x 10^{11} cm^{-2}, respectively). A marginal degradation of microstructural parameters is seen in epilayers grown at higher substrate temperatures, due to the dominance of 3D hillock type growth.

Keywords: Zinc oxide, reactive sputtering, epitaxy, high resolution x-ray diffraction

1. Introduction

Epitaxial zinc oxide (ZnO) films have attracted considerable interest due to their potential applications in transparent electronics and short wavelength optoelectronic devices [1, 2]. Hetero-epitaxial ZnO films have usually been grown on sapphire, in spite of the large lattice mismatch (~ 18 %), primarily due to its availability as large area wafer and low cost, but is also driven by the similarities in the structures of ZnO and GaN and the fact that sapphire substrates are routinely used for GaN based devices. High quality ZnO epilayers have been usually deposited by molecular beam epitaxy (MBE), pulsed laser deposition (PLD), and metalorganic chemical vapor deposition (MOCVD) [1-3]. Sputtering is an attractive alternative due to its low substrate temperature requirement, amenability to large area deposition, scalability and low cost, which has also been explored for the growth of epitaxial ZnO films on c-plane sapphire [4-10]. In view of the strong influence that microstructure of epilayers has on their electrical and optical properties, the evolution of microstructure of sputtered ZnO epilayers on c-plane sapphire has been studied earlier by some groups [4-9].

Park *et al.* used real-time synchrotron x-ray scattering to study the growth mode of ZnO epilayers on sapphire at a substrate temperature of 300 °C and observed the growth of highly strained and well aligned 2D layer up to a thickness of 4.5 nm. 2D-3D mixed mode of growth was observed up to a thickness of 18 nm, beyond which only 3D columnar grains were found to grow [4]. Kim *et al.* [5] also studied the temperature dependence of the growth mode of 2-140 nm thick sputtered ZnO/Al_2O_3 by x-ray scattering and have shown that the growth mode changes from 2D layer to 3D islands as the temperature increased from 300 °C to 600 °C, with the prevalence of 2D platelet type growth at intermediate temperatures. Seo *et al.* have also studied the effect of rf power and substrate temperature (400 - 650 °C) on the heteroepitaxial growth of

ZnO/sapphire and found that the strain relaxation was independent of rf power but was highly dependent on the substrate temperature [6]. Singh *et al.* have studied the microstructural parameters of ~ 500 nm thick ZnO epilayers grown on sapphire at 300 °C and 600 °C and found a significant improvement of microstructure at the higher substrate temperature [7]. Ruthe *et al.* have studied the low temperature epitaxy of 400 - 1000 nm thick ZnO on sapphire with ω-scan and ϕ-scan measurements. They have shown that the epitaxial relationship between ZnO and sapphire was maintained down to 80 °C, although the crystalline quality detoriated with decrease of substrate temperature. They have also shown that the crystalline quality degraded at higher oxygen/zinc flux and power [8]. Yu *et al.* have also demonstrated the epitaxial growth of ZnO/c-sapphire films at low substrate temperature of 150 ℃ and observed that most of the strain was released as the film thickness reached about 80 nm [9].

The above studies have shown interesting heteroepitaxial growth behavior of ZnO on c-sapphire by sputtering. Apart from the demonstration of epitaxial growth at moderate substrate temperatures, study of the evolution of strain with film thickness reveals that the mode of growth changes from 2D to 3D during the early stages and depends significantly on substrate temperature. Although, sputtering is the most extensively used technique for the growth of ZnO films, studies of the epitaxial growth of ZnO by reactive sputtering have been rather limited [7-9]. The present work attempts a comprehensive microstructural investigation of reactively sputtered ZnO epilayers on c-sapphire by high resolution x-ray diffraction (HRXRD). ZnO epilayers of thickness in the range of 25-200 nm were grown at low and moderate substrate temperatures of 100-500 °C and their microstructural parameters, namely, coherence lengths, micro-strain, crystallite tilt and twist and the corresponding densities of edge and screw dislocations were obtained. These parameters display a systematic dependence on

substrate temperature and thickness of the epilayers and thus provide interesting insight into the growth behavior of sputtered ZnO epilayers on sapphire.

2. Experimental Details

ZnO films were deposited on c-sapphire substrates (of size 12 mm x 12 mm) by reactive rf magnetron sputtering of a Zn target in 20% O_2-Ar mixture. Prior to deposition, sapphire substrates were cleaned with organic solvents followed by ultrasonic rinsing with de-ionized water. Subsequently, the substrates were subjected to RCA-1 treatment by heating in a 2:1 mixture of H_2O:NH_4OH up to 80 °C and then adding one part H_2O_2 solution, followed by further heating for 15 min. This was followed by ultrasonic rinsing in deionized water, acetone, and propanol and finally degreasing in propanol vapor. The rf power was 400W and the deposition was carried out at a pressure of 10^{-2} mbar. More details of the deposition process have been described elsewhere [7]. ZnO films grown with nominal thickness, 25, 50, 100 and 200 nm (at 300 °C) and in the substrate temperature range of 100 - 500 °C (with 100 nm thickness) were deposited on c-plane sapphire substrates. The thickness of the film was measured by Ambios XP-2 surface profilometer and the uniformity was found to be within ±5%. The deposition rates were typically in the range of 15-20 nm/min. Powder X-ray diffraction (XRD) measurements were carried out with Cu-Kα1 radiation followed by detailed HRXRD measurements in phi (ϕ), omega (ω) and ω-2θ scan geometries, using a PANalytical X'Pert MRD system. The incident beam optics had a 4-bounce hybrid monochromator, which ensured Cu-Kα1 output collimated to about 20 arcsecs in the plane of scattering. A ½ deg slit was placed at the output before the detector.

3. Results

ZnO films of different thickness (in the range of 25 - 200 nm) were deposited on sapphire substrate at a temperature of 300 °C. Another set of ~ 100 nm thick ZnO films were deposited at different substrate temperatures in the range of 100 - 500 °C. The structure of the films was studied by powder XRD and a typical XRD pattern of a 100 nm thick ZnO film deposited at 300 °C is shown in Fig. 1. All the films exhibited the hexagonal wurtzite structure of ZnO (JCPDS File No. 36-1451) and showed a single low angle (0002) peak in the 2θ range of 31° - 37°, in which, the prominent ZnO peaks due to $(10\bar{1}0)$, (0002) and $(10\bar{1}1)$ reflections are expected. The crystallite size (calculated from Scherrer formula) along the growth direction (c-axis) was in the range of (30 - 40) nm and increased marginally for thicker (> 100 nm) films, particularly those deposited at higher temperatures. The films deposited at and below 300 °C displayed c-values of 0.523 ± 0.001 nm, which was slightly larger than the standard c-value of 0.5205 nm. For films deposited above 300 °C the c-values were found to be close to the standard value, indicating negligible lattice strain. Thus, the films deposited at and below 300 °C, displayed a lattice strain ($\Delta c/c$) of 5 x 10^{-3}, which corresponds to in-plane compressive stress [11] of - 0.8 GPa. The in-plane stress was estimated to be less than ± 0.1 GPa for the films deposited above 300 °C. This behavior is indicative of the stress being intrinsic in origin, possibly due to bombardment of the growing film by O^- ions, which has been reported [12] to cause compressive stress.

The ϕ-scans of asymmetric $(10\bar{1}1)$ reflection were carried out for ZnO films of different thickness as well as those deposited at different substrate temperatures. Fig. 2 (a) shows the ϕ-scans of the ZnO films of different thickness (deposited at 300 °C), which also includes the ϕ-scan of $(10\bar{1}4)$ reflection of the sapphire substrate. In all the

cases, the ϕ-scans show the presence of six dominant peaks at 60° with each other, revealing the six fold symmetry of the hexagonal lattice. This is indicative of the in-plane orientation of crystallites and an evidence of the epitaxial growth of ZnO films on sapphire substrates. Comparison of the ϕ-scans of ZnO films with that of the sapphire substrate shows that ZnO lattice is rotated by 30° with respect to the sapphire lattice, exhibiting an in-plane epitaxial relationship ZnO $[10\bar{1}0] \parallel \alpha\text{-}Al_2O_3[11\bar{2}0]$, as reported earlier [13, 14]. Fig. 2 (b) shows the ϕ-scans for ~ 100 nm thick ZnO films deposited at different substrate temperatures, which also includes the ϕ-scan of $(10\bar{1}4)$ reflections of the sapphire substrate. The ϕ-scans of ZnO films deposited at relatively lower temperatures of 100 °C and 200 °C, show weak and broad $(10\bar{1}1)$ reflections, possibly with some additional peaks, indicating the presence of misaligned crystallites and poor in-plane crystallinity. In contrast, the ZnO films deposited at higher substrate temperatures of 300 - 600 °C show sharp $(10\bar{1}1)$ reflections with six fold symmetry, indicating a much improved mosaic structure and epitaxial quality.

The microstructure and epitaxial quality of the above described ZnO epilayers have been studied by ω and ω-2θ scans. Epitaxial films grown on lattice-mismatched substrates consist of oriented mosaic blocks, having certain average dimensions along the growth direction (vertical coherence length) and in the growth plane (lateral coherence length). The mosaic blocks can also be slightly mis-oriented with respect to each other. The mis-orientation of the mosaic blocks out of the sample plane and within the sample plane are represented by crystallite tilt and crystallite twist, respectively. The finite lateral coherence length (LCL) and tilt of the mosaic blocks cause broadening (Δq_x) of (000*l*) reflections in ω-scans [15]. These parameters have been respectively estimated from the intercept and slope of the corresponding Williamson–Hall plots of Δq_x (FWHM along q_x direction) vs. q, the magnitude of (000*l*) point in

reciprocal space. Similarly, the finite vertical coherence length (VCL) and micro-strain cause a broadening (Δq_z) of (000*l*) reflections in the ω-2θ scan [15]. These parameters have been respectively estimated from the intercept and slope of the corresponding Williamson–Hall plots of Δq_z (FWHM along q_z direction) vs. q. For highly c-axis oriented films, the in-plane mis-orientation of mosaic blocks or crystallite twist can be approximately measured from the FWHM of the reflection from an asymmetric plane, which is suitably oriented with respect to the (0002) plane [16]. In this work, the FWHM of the ω-scan of $(10\bar{1}1)$ reflection has been used to estimate the crystallite twist for the ZnO epilayers. It is known that in wurtzite systems, pure edge and pure screw dislocations dominate over mixed type of dislocations [17, 18]. The pure-screw type dislocations in wurtzite system are along [0001] direction with Burger's vector <0001>. The pure-edge-type dislocations are also along [0001] direction, but with Burger's vector (1/3) <1120>. Assuming a random distribution of these dislocations, the values of crystallite tilt and twist were used to estimate the densities of screw and edge dislocations, respectively, following the approach of References [19] and [20]. The dislocation densities (N) have thus been estimated from the expression: $N=\alpha^2/4.35b^2$, where α is the value of tilt/twist and b is the corresponding magnitude of Burger's vector. These results are described below.

The ω-scans for symmetric (0002), (0004) and (0006) reflections of ZnO epilayers of different thickness deposited at 300 °C are shown in Fig. 3(a) and the corresponding Williamson–Hall plots are shown in Fig. 3(c). The ω-scans for 100 nm thick epilayers deposited at different substrate temperatures are shown in Fig. 3(b) and the corresponding Williamson–Hall plots are shown in Fig. 3(d). The ω-scans of (0002) reflection exhibit a narrow peak superimposed over a broad peak for the 25 nm and 50 nm thick ZnO epilayers deposited at 300 °C (Fig. 3(a)) as well as in the case of the 100

nm thick ZnO epilayer deposited at 100 °C (Fig. 3(b)). This feature is attributed to the initial growth of a highly strained and aligned 2D layer of ZnO on sapphire, in spite of the ~ 18% lattice mismatch between ZnO and sapphire, as has been reported earlier [4, 5]. For the ZnO epilayers of different thickness grown at 300 °C, the variation of LCL and crystallite tilt with thickness is given in Table 1(a). It is seen that the 25 nm thick epilayer has a small LCL value of 60 nm, whereas the thicker epilayers display larger and nearly similar LCL values of 165-185 nm. The crystallite tilt decreases from ~ 1.1° to 0.74°, as the thickness of the epilayer increases from 25 nm to 100 nm, but with increase of thickness to 200 nm, the crystallite tilt again increases to a value of 1.14°. The variation of LCL and crystallite tilt with substrate temperature for 100 nm thick epilayer is given in Table 1(b). It may be mentioned that the common data for the 100 nm thick epilayer grown at 300 °C is included in both Tables 1(a) and 1(b) for easy comparison. The ZnO epilayer grown at 100 °C displays a large LCL value of ~ 900 nm, which decreases drastically to ~ 100 nm with increase in substrate temperature. The crystallite tilt decreases from 1.1° to 0.74° with increase in substrate temperature from 100 °C to 300 °C, but increases again to 1.0° with further increase in substrate temperature to 500 °C.

The ω-2θ scans for symmetric (0002), (0004) and (0006) reflections of ZnO epilayers of different thickness deposited at 300 °C are shown in Fig. 4(a) and corresponding Williamson–Hall plots are shown in Fig. 4(c). The ω-2θ scans for 100 nm thick epilayers deposited at different substrate temperatures are shown in Fig. 4(b) and the corresponding Williamson–Hall plots are shown in Fig. 4 (d). Table 1(a) and 1(b) show that the VCL values increase monotonously with increase in thickness and are comparable to the thickness of epilayers, irrespective of the substrate temperature. It is also seen from Table 1(a) that the 25 nm thick epilayer exhibits a micro-strain of 4.6

× 10^{-3}, which decreases significantly to 1.2 × 10^{-3} for the 100 nm thick epilayer. However, a large increase in micro-strain to 3.6 × 10^{-3} is observed for the 200 nm thick epilayer. Table 1(b) shows that the 100 nm thick ZnO epilayer deposited at 100 °C displays a large micro-strain of 4.4 × 10^{-3}, which decreases substantially to 1.2 × 10^{-3} for the epilayer deposited at 300 °C. Further increase in substrate temperature to 500 °C, however, results in a small increase in the value of micro-strain to 1.7 × 10^{-3}.

The ω-scans of $(10\bar{1}1)$ reflection of ZnO epilayers of different thickness grown at 300 °C are shown in Fig. 5(a) and those for 100 nm thick epilayers grown at different substrate temperatures are shown in Fig. 5(b). The corresponding data in Table 1(a) shows that the crystallite twist has a value of 1.26° for the 100 nm thick ZnO epilayer, which is substantially smaller than the twist values of 2° - 4°, observed for both thinner and thicker epilayers. Table 1(b) shows that the crystallite twist of the epilayers deposited at 100 °C and 500 °C also exhibit larger values of 4.4° and 1.8° respectively, compared to the twist value for the epilayer deposited at 300 °C. As mentioned above, the crystallite tilt and twist data have been used to estimate the densities of screw and edge dislocations, respectively and these values are also listed in Tables 1(a) and 1(b). It is found from Table 1(a) that among the different epilayers of thickness ranging from 25 nm to 200 nm grown at 300 °C, the 25 nm thick epilayer displays the highest density of edge dislocations (8.1 × 10^{11} cm^{-2}). The density of edge dislocations decreases with increase of thickness to a value of 1.1 × 10^{11} cm^{-2} for the 100 nm thick epilayer, but increases with further increase in thickness to reach a value of 3.8 × 10^{11} cm^{-2} for the 200 nm thick epilayer. The density of screw dislocations also decreases initially with increase in thickness of the epilayer from 25 nm to 100 nm, exhibiting a minimum value of 1.4 × 10^{10} cm^{-2} as shown in Table 1(a). However, with further increase in thickness to 200 nm, the density of edge dislocation increases to 3.0 × 10^{10} cm^{-2}.

Similarly, the data presented in Table 1(b) shows that the 100 nm thick epilayer deposited at substrate temperature of 100 °C displays a high density of edge dislocations (1.3×10^{12} cm^{-2}), which decreases substantially to 1.1×10^{11} cm^{-2} and 2.1×10^{11} cm^{-2} for the epilayers deposited at substrate temperatures of 300 °C and 500 °C, respectively. Table 1(b) also shows that the density of screw dislocations for the epilayer deposited at 100 °C is 3.1×10^{10} cm^{-2}, which decrease to 1.4×10^{10} cm^{-2} for the epilayer deposited at 300 °C. However, with further increase of substrate temperature to 500 °C, the density of screw dislocations increases marginally to 2.4×10^{10} cm^{-2}.

The microstructural parameters summarized above in Table 1(a) and 1(b) show that the sputtered ZnO epilayers of thickness ~ 100 nm deposited at 300 °C exhibit superior microstructural parameters, including the lowest values of micro-strain (1.2×10^{-3}) and edge (1.1×10^{11} cm^{-2}) and screw (1.4×10^{10} cm^{-2}) dislocation densities. Before discussing the dependence of the epitaxial growth behavior on thickness and substrate temperature, it is interesting to note that the above values of dislocation densities are quite comparable to the corresponding values reported for ZnO epilayers obtained by different techniques [7, 21-26], particularly those grown at substrate temperatures of ~ 500 °C or lower, without a buffer layer. For example, ZnO epilayers grown by MBE below 500 °C, exhibit the density of dislocations in the range of (1-7) x 10^{10} cm^{-2} [21, 22] as reported by high-resolution transmission electron microscopy (TEM) studies. However, in the case of ZnO epilayers grown by MBE at 700 °C, smaller dislocation densities in the range of (3-7) x 10^{10} cm^{-2} have been reported [23]. Zhou *et al.* [24] have used HRXRD to obtain the values of screw and edge dislocation densities of ~ 3.8 x 10^{9} cm^{-2} and ~ 1.4 x 10^{11} cm^{-2}, respectively, for plasma enhanced chemical vapor deposited epitaxial ZnO films on sapphire. In the case of PLD grown

ZnO epilayers at 600 °C on sapphire, relatively smaller values of screw and edge dislocation densities of ~ 2.5 x 10^8 cm^{-2} and 1.6 x $10^{10}cm^{-2}$, respectively, have been reported [25], based on TEM measurements. Narayan *et al.*[26] have also shown by TEM measurements that ~250 nm thick ZnO epilayers grown at ~ 800 °C by PLD exhibit a dislocation density of ~ 2 x 10^{10} cm^{-2} near the interface, which decreases to ~ 10^7 cm^{-2} on the surface of the epilayer.

4. Discussion

The above results show that reactively sputtered ZnO grows epitaxially on c-sapphire in a moderate temperature range, which is attributed to the presence of energetic species, reducing significant dependence on substrate temperature. However, these studies also reveal that both substrate temperature and thickness play a critical role in determining the quality of epitaxy. The ZnO epilayer of thickness ~ 100 nm grown at a substrate temperature of ~ 300 °C has been found to yield the best microstructural parameters. The quality of epitaxy is observed to deteriorate for thinner and thicker epilayers as well as for those grown at lower and higher substrate temperatures. These features are discussed below.

The results presented in Figs. 2(a) – 5(a) and those summarized in Table 1(a) show that the microstructural parameters of ZnO epilayers grown at a substrate temperature of ~ 300 °C, exhibit a strong dependence on thickness in the range of 25 - 200 nm. In the cases of 25 nm and 50 nm thick epilayers, the appearance of a narrow peak superimposed over a broad ω-scan peak of (0002) reflection (Fig. 3(a)) is indicative of the initial growth of a strained 2D layer. The sharp ϕ-scan peaks in Fig. 2(a), displaying six fold symmetry also support the presence of a laterally aligned 2D layer in these cases. It is also clear that the strain relaxation and consequent transition to an energetically favorable mode of growth takes place at a thickness well below 25 nm,

which is consistent with earlier reports [4, 5]. However, Table 1(a) shows that the thinner epilayers (25 nm and 50 nm) display poor micro-structural parameters which are attributed to the transition from highly strained 2D layer type growth, the nature of which will be discussed in more detail below. The transition introduces crystallographic defects which propagate into subsequent growth resulting in relatively larger dislocation densities in these cases.

An interesting observation is noted from Fig. 3(b), which shows the presence of a prominent narrow peak over the broad ω-scan peak of (0002) reflection for the relatively thicker (100 nm) epilayer grown at 100 °C. Such a peak is clearly absent in the cases of epilayers of the same thickness grown at 300 °C and 500 °C. Another relevant observation is the large value of LCL (~ 900 nm) seen in this case (Table 1(b)). These observations suggest that at lower substrate temperatures, the 2D growth mode prevails up to relatively larger thickness, or in other words, the transition from 2D mode of growth takes place at lower thickness, as the substrate temperature is increase. This is understandable, as at lower substrate temperatures, absence of sufficient surface diffusion restricts the re-arrangement of the material into 3D hillocks and hence, the consequent transition to 3D growth mode [27].

Coming back to the effect of thickness on the epilyers grown at 300 °C, it is observed from Table 1(a) that the epilayers of thickness ~ 100 nm or more exhibit much improved microstructural parameters, particularly, smaller micro-strain and dislocation densities, compared to 25 - 50 nm thick epilayers. This is essentially attributed to the marginalization of the effect of the 2D strained layer in determining the overall microstructural quality of thicker epilayers Interestingly, Table 1(a) also shows that with further increase in thickness to 200 nm, the epilayer exhibits relatively inferior microstructural parameters, particularly in terms of micro-strain and dislocation

densities, which may be indicative of the increase in misalignment of mosaic blocks or 3D crystallites in thick epilayers.

The effect of substrate temperature on the microstructure of 100 nm thick epilayer can be seen in Figs. 2(b) – 5(b). The poor ϕ-scan features of the epilayers grown at lower substrate temperatures of 100 °C and 200 °C (Fig. 2(b)) and their much inferior microstructural parameters (Table 1(b)) are attributed to the poor quality of epitaxy that takes place at lower substrate temperatures due to the delayed 2D - 3D transition (at larger thickness), as explained above. With increase in substrate temperature to 300 °C, the 100 nm thick ZnO epilayer displays significant improvement in all the microstructural parameters, as seen from Table 1(b), particularly the decrease in micro-strain and density of edge dislocations, which are the dominant threading dislocations in wurtzite systems like ZnO [28]. The improvement of microstructural parameters at 300 °C is in agreement with the observations of Kim et.al. [5], who invoked the prevalence of 2D platelet type growth behavior. They have proposed that at intermediate substrate temperatures, owing to increased surface diffusion and intermediate ad-atom mobility [29], 2D platelets are formed with intermediate strain and the ad-atoms are incorporated into the edge sites as well as over the platelets [30]. The absence of the sharp superimposed ω-scan peak in the case of 100 nm thick epilayer grown at 300 °C and its substantially smaller micro-strain, compared to the thinner epilayers, thus indicate that the strain relaxation takes place through the formation of 2D platelets over which 3D islands grow at moderate substrate temperatures. Interestingly, with increase of substrate temperature to 500 °C, a noticeable degradation of microstructural parameters of the 100 nm thick epilayer is seen from Table 1(b). This is attributed to the prevalence of strain relaxed 3D hillock

type growth due to enhanced surface diffusion available at higher substrate temperatures and the consequent misalignment of the mosaic blocks.

5. Conclusions

This work deals with a quantitative estimation of the micro-structural parameters of sputtered ZnO epilayers grown on c-sapphire in the range of 100 – 500 °C. It is demonstrated that substrate temperature and thickness of the epilayer have interrelated effects on the quality of epitaxy and micro-structural properties of the epilayers. At lower substrate temperatures of 100 - 200 °C, poor quality epitaxy is observed, which is primarily attributed to the initial growth of a strained 2D layer and subsequent changes in growth behavior, which lead to the formation of crystallographic defects. With increase in substrate temperature to 300 °C, owing to enhanced surface diffusion and ad-atom mobility, strain relaxation takes place by a transition from 2D growth to platelet type growth with intermediate strain, together with the shift of this transition to lower thicknesses. The consequent marginalization of the effect of the strained 2D layer and the partially strain-relaxed growth of 3D islands over 2D platelets result in the substantial improvement seen in the microstructural parameters of relatively thick epilayers (~ 100 nm) grown at moderate substrate temperatures (~ 300 °C). These parameters include, micro-strain of ~ 1.2 x 10^{-3} as well as screw and edge dislocation densities of ~ 1.4 x 10^{10} cm^{-2} and ~ 1.1 x 10^{11} cm^{-2}, respectively, which are comparable to those reported for ZnO epilayers grown by several other techniques at relatively low substrate temperatures. A marginal degradation of the microstructural parameters of ZnO epilayers is observed at higher substrate temperatures, which is attributed to the availability of sufficient surface diffusion, which facilitates the energetically favorable 3D hillock type growth. This study provides relevant inputs for

the application of epitaxial ZnO films, which may be particularly useful for the low temperature processing of ZnO-based transparent electronic and optoelectronic devices.

Acknowledgements

The authors would like to thank Prof. Raman Srinivasa for his keen interest in this work and helpful discussions.

References

[1] Ozgur U, Alivov Y I, Liu C, Teke A, Reshchikov M A, Dogan S, Avrutin V, Cho S J and Morkoc H 2005 A comprehensive review of ZnO materials and devices *J. Appl. Phys.* **98** 041301-103.

[2] Morkoc H and Ozgur U 2007 *Zinc Oxide - Fundamentals, Materials and Device Technology* (Weinhiem, Germany: Wiley-VCH Verlag GmbH & Co).

[3] Triboulet R and Perriere J 2003 Epitaxial growth of ZnO films *Progress in Crystal Growth and Characterization of Materials* **47** 65-138.

[4] Park S I, Cho T S, Doh S J, Lee J L and Je J H 2000 Structural evolution of ZnO/sapphire (001) heteroepitaxy studied by real time synchrotron x-ray scattering *Appl. Phys. Lett.* **77** 349-51.

[5] Kim I W and Lee K M 2008 Temperature dependence of microstructure and strain evolution in strained ZnO films on Al_2O_3 (0001) *Nanotechnology* **19** 355709-16.

[6] Seo S H and Kang H C 2010 Growth of ZnO/sapphire heteroepitaxial thin films by radio-frequency sputtering with a raw powder target *Thin Solid Films* **518** 5164-8.

[7] Singh S, Kumar R, Ganguli T, Srinivasa R S and Major S S 2008 High optical quality ZnO epilayers grown on sapphire substrates by reactive magnetron sputtering of zinc target *J. Crys. Growth* **310** 4640-6.

[8] Ruthe K C, Cohen D J and Barnett S A 2004 Low temperature epitaxy of reactively sputtered ZnO on sapphire *J. Vac. Sci. Tech. A* **22** 2446-52.

[9] Yu C J, Sung N E, Lee H K, Shin H J, Yun Y D, Kang S W and Lee I J 2011 Structural properties of low-temperature grown ZnO thin films determined by X-ray diffraction and X-ray absorption spectroscopy *Thin Solid Films* **519** 4366-70.

[10] Jeong S H, Kim I S, Kim S S, Kim J K and Lee B T 2004 Homo-buffer layer effects and single crystalline ZnO hetero-epitaxy on c-plane sapphire by a conventional RF magnetron sputtering *J. Crys. Growth* **264** 110-5.

[11] Ohring M 2002 *Materials Science of Thin Films Deposition and Structure* (Chapter 12, Cambridge, USA: Academic Press).

[12] Kappertz O, Drese R and Wuttig R 2002 Correlation between structure, stress and deposition parameters in direct current sputtered zinc oxide films *J. Vac. Sci. Technol. A* **20** 2084-95.

[13] Fons P, Iwata K, Niki S, Yamada A and Matsubara K 1999 Growth of high-quality epitaxial ZnO films on α-Al_2O_3 *J. Cryst. Growth* **201-202**, 627-32.

[14] Chen Y, Bagnall D M, Koh H J, Park K T, Hiraga K, Zhu Z Q and Yao T 1998 Plasma assisted molecular beam epitaxy of ZnO on c -plane sapphire: Growth and characterization *J. Appl. Phys*. **84** 3912-18.

[15] Chierchia R, Bottcher T, Heinke H, Einfeldt S, Figge S and Hommel D, 2003 Microstructure of heteroepitaxial GaN revealed by x-ray diffraction *J. Appl. Phys.* **93,** 8918-25.

[16] Hong S K, Ko H J, Chen Y and Yao T 2002 Control of ZnO film polarity *J. Vac. Sci. Technol. B* **20** 1656-63.

[17] Zhang B P, Wakatsuki K, Binh N T, Usami N and Segawa Y 2004 Effects of growth temperature on the characteristics of ZnO epitaxial films deposited by metalorganic chemical vapor deposition *Thin Solid Films* **449** 12-19.

[18] Srikant V, Speck J S and Clarke D R 1997 Mosaic structure in epitaxial thin films having large lattice mismatch *J. Appl. Phys.* **82** 4286-95.

[19] Metzger T, Hopler R, Born E, Ambacher O, Stutzmann M, Strommer R, Schuster M, Gobel H, Christiansen S, Albrecht M and Strunk H P 1998 Defect structure of epitaxial GaN films determined by transmission electron microscopy and triple-axis X-ray diffractometry *Phil. Mag. A* **77** 1013-25.

[20] Gay P, Hirsch P B and Kelly A 1953 The estimation of dislocation densities in metals from X-ray data *Acta Metall.* **1** 315-19.

[21] Vigué F, Vennéguès P, Deparis C, Vézian S, Laügt M and Faurie J P 2001 Growth modes and microstructures of ZnO layers deposited by plasma-assisted molecular-beam epitaxy on (0001) sapphire *J. Appl. Phys.* **90** 5115-9.

[22] Vennéguès P, Chauveau J M, Korytov M, Deparis C, Zuniga-Perez J and Morhain C 2008 Interfacial structure and defect analysis of nonpolar ZnO films grown on R-plane sapphire by molecular beam epitaxy *J. Appl. Phys.* **103** 083525-32.

[23] A. Setiawan A, Vashaei Z, Cho M W, Yao T, Kato H, Sano M, Miyamoto K, Yonenaga I and Ko H J 2004 Characteristics of dislocations in ZnO layers grown

by plasma-assisted molecular beam epitaxy under different Zn/O flux ratios *J. Appl. Phys.* **96** 3763-8.

[24] Zhou S, Wu M F, Yao S D, Lu Y M and Liu Y C 2006 The strain reduction and quality improvement in ZnO film by a 30^{o} in-plane rotation with respect to the Al_2O_3 substrate *Mater. Res. Bull.* **41** 2198-203.

[25] Liu W R, Hsieh W F, Hsu C H, Liang K S and Chien F S S 2006 Influence of the threading dislocations on the electrical properties in epitaxial ZnO thin films *J. Cryst. Growth* **297** 294-9.

[26] Narayan J, Dovidenko K, Sharma A K and Oktyabrsky S 1998 Defects and interfaces in epitaxial ZnO/α-Al_2O_3 and AlN/ZnO/α- Al_2O_3 heterostructures *J. Appl. Phys.* **84** 2597-601.

[27] Smith D 1995 *Thin Film Deposition: Principles & Practice* (N.J., USA: McGraw Hill Education).

[28] Ayers J E 2007 *Heteroepitaxy of Semiconductors: Theory, Growth, and Characterization* (C.T., USA: CRC Press, Taylor & Francis Group).

[29] Mula G, Adelmann C, Moehl S, Oullier J and Daudin B 2001 Surfactant effect of gallium during molecular-beam epitaxy of GaN on AlN (0001) *Phys. Rev. B* **64** 195406-18.

[30] Markov I V 1995 *Crystal Growth for Beginners* (Chapter 4, Singapore: World Scientific).

List of figure and table captions

Fig.1. Powder X-ray diffraction patterns of a typical ZnO film of ~ 100 nm thickness grown on sapphire at a substrate temperature of 300 °C.

Fig. 2. (a) ϕ-scans of $(10\bar{1}1)$ reflections of ZnO epilayers of different thicknesses(as indicated in the figure) grown on sapphire at 300 °C and (b) ϕ-scans of $(10\bar{1}1)$ reflections of 100 nm thick ZnO epilayers grown on sapphire at different substrate temperatures (as indicated in the figure). The ϕ-scans of $(10\bar{1}4)$ reflections of sapphire substrate are also given in both cases.

Fig. 3. The ω-scans of (0002), (0004) and (0006) reflections for (a) ZnO epilayers of different thicknesses (as indicated in the figure) grown on sapphire at 300 °C and (b) 100 nm thick ZnO epilayers grown on sapphire at different substrate temperatures (as indicated in the figure) . The corresponding Williamson – Hall plots (Δq_x vs. q) for (0002), (0004) and (0006) reflections are presented in Figs. 3(c) and 3(d), respectively.

Fig. 4.The ω-2θ scans of (0002), (0004) and (0006) reflections for (a) ZnO epilayers of different thicknesses (as indicated in the figure) grown on sapphire at 300 °C and (b) 100 nm thick ZnO epilayers grown on sapphire at different substrate temperatures (as indicated in the figure). The corresponding Williamson – Hall plots (Δq_z vs. q) for (0002), (0004) and (0006) reflections are presented in Figs. 4(c) and 4(d), respectively.

Fig. 5. The ω-scans of $(10\bar{1}1)$ reflection for (a) ZnO epilayers of different thicknesses (as indicated in the figure) grown on sapphire at 300 °C and (b) 100 nm thick ZnO epilayers grown on sapphire at different substrate temperatures (as indicated in the figure).

Table 1(a). Micro-structural parameters of ZnO epilayers of different thicknesses grown on sapphire substrates at 300 °C.

Thickness (nm)	Intercept ($1/\Delta q_x$) LCL (nm)	Tilt (deg)	Intercept ($1/\Delta q_z$) VCL (nm)	Micro strain	Twist (deg)	Dislocation Density	
						Screw (cm^{-2})	Edge (cm^{-2})
25	60	1.08	30	4.6×10^{-3}	3.50	3.0×10^{10}	8.1×10^{11}
50	170	0.88	60	3.5×10^{-3}	2.03	2.0×10^{10}	2.7×10^{11}
100	165	0.74	65	1.2×10^{-3}	1.26	1.4×10^{10}	1.1×10^{11}
200	185	1.14	160	3.6×10^{-3}	2.39	3.0×10^{10}	3.8×10^{11}

Table 1(b). Micro-structural parameters of 100 nm thick ZnO epilayers grown on sapphire at different substrate temperatures.

Substrate Temperature (^oC)	Intercept ($1/\Delta q_x$) LCL (nm)	Tilt (deg)	Intercept ($1/\Delta q_z$) VCL (nm)	Micro strain	Twist (deg)	Dislocation Density	
						Screw (cm^{-2})	Edge (cm^{-2})
100 °C	900	1.1	110	4.4×10^{-3}	4.4	3.1×10^{10}	1.3×10^{12}
300 °C	165	0.74	65	1.2×10^{-3}	1.26	1.4×10^{10}	1.1×10^{11}
500 °C	100	1.0	60	1.7×10^{-3}	1.8	2.4×10^{10}	2.1×10^{11}

Fig 1.

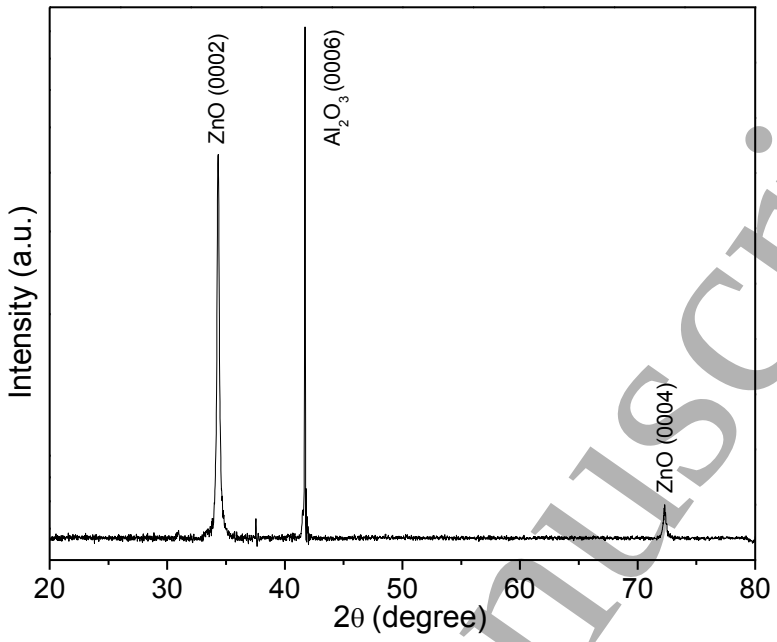

Fig 2.

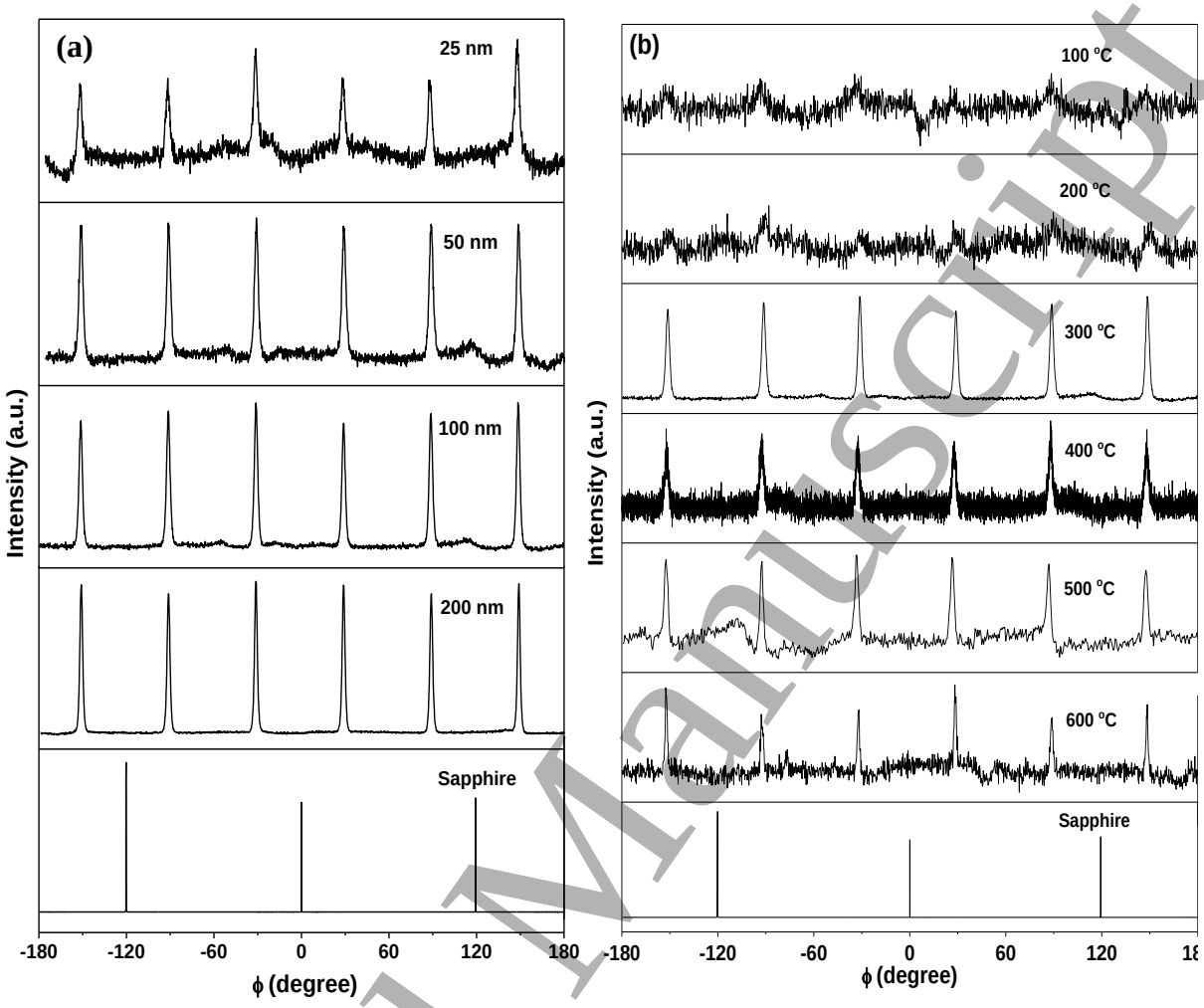

Fig 3. (a & b)

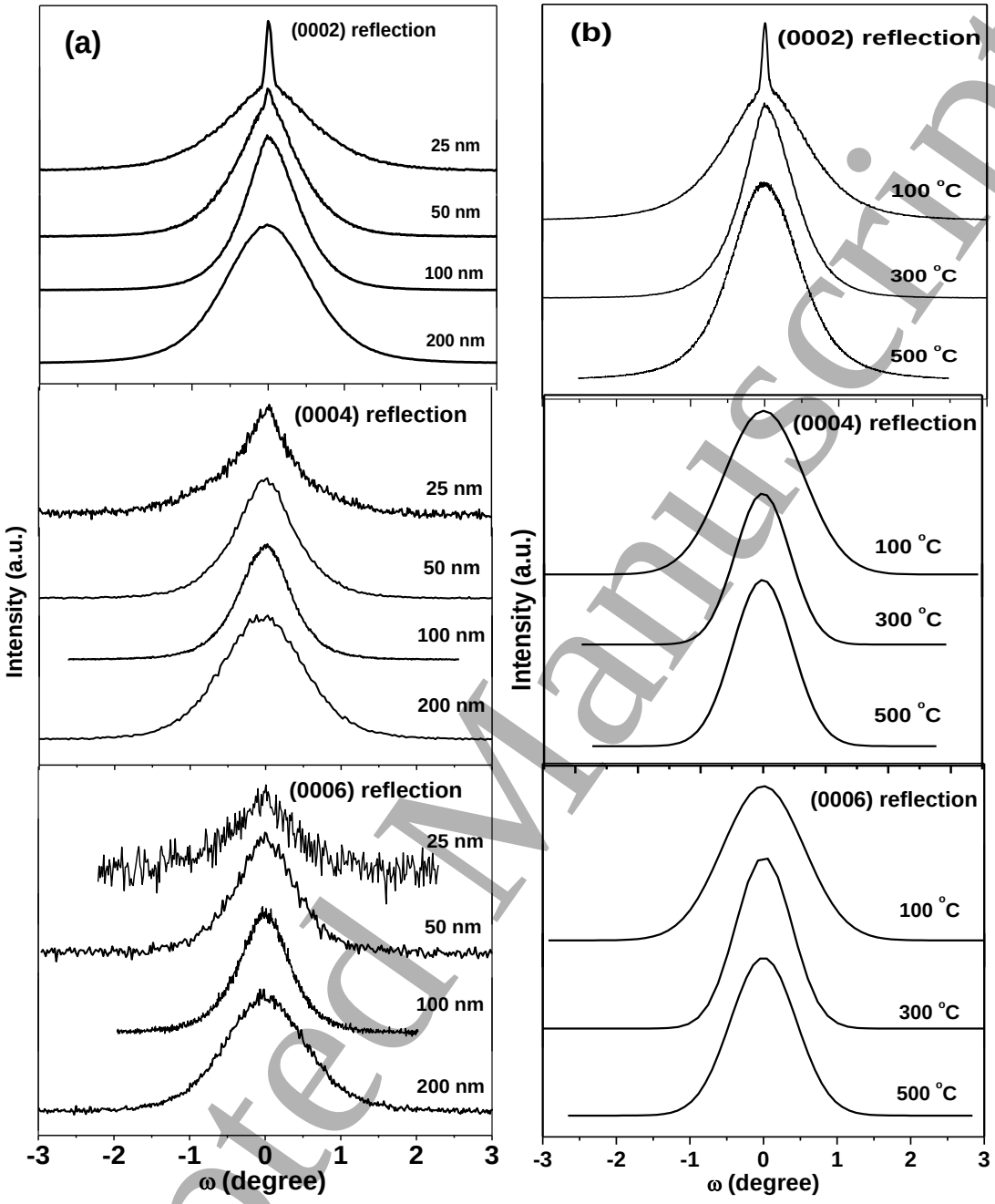

Fig 3. (c & d)

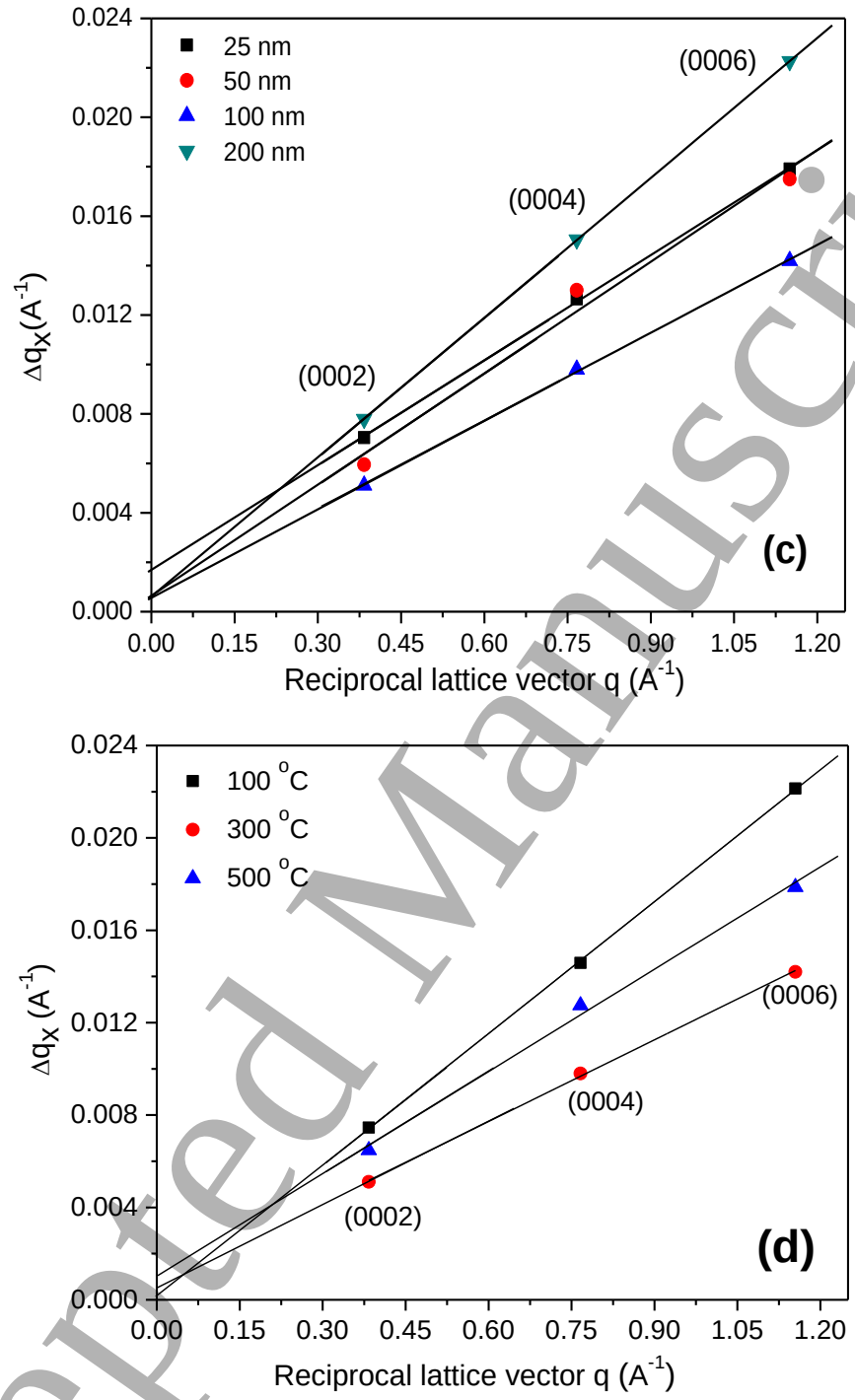

Fig 4. (a & b)

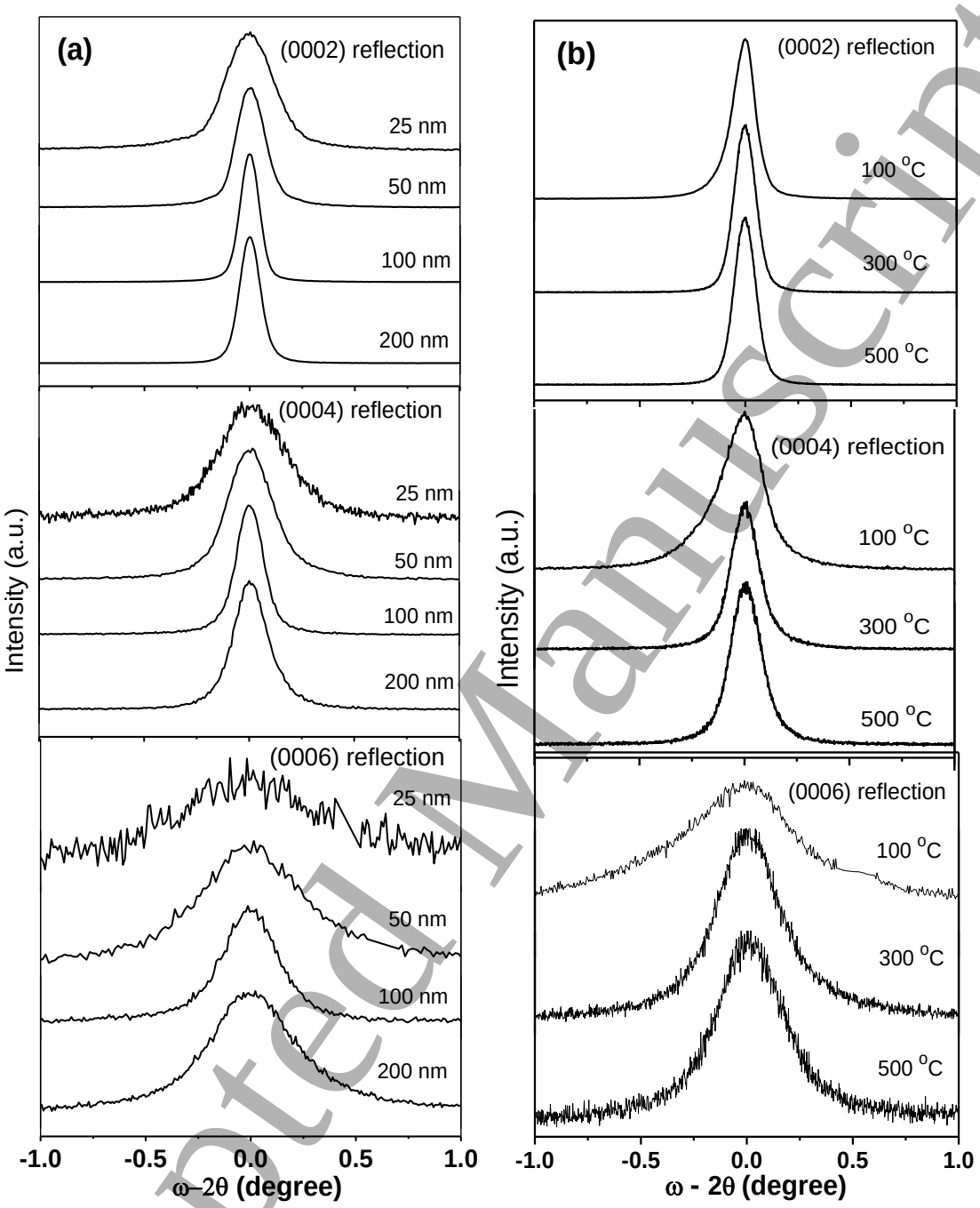

Fig 4. (c & d)

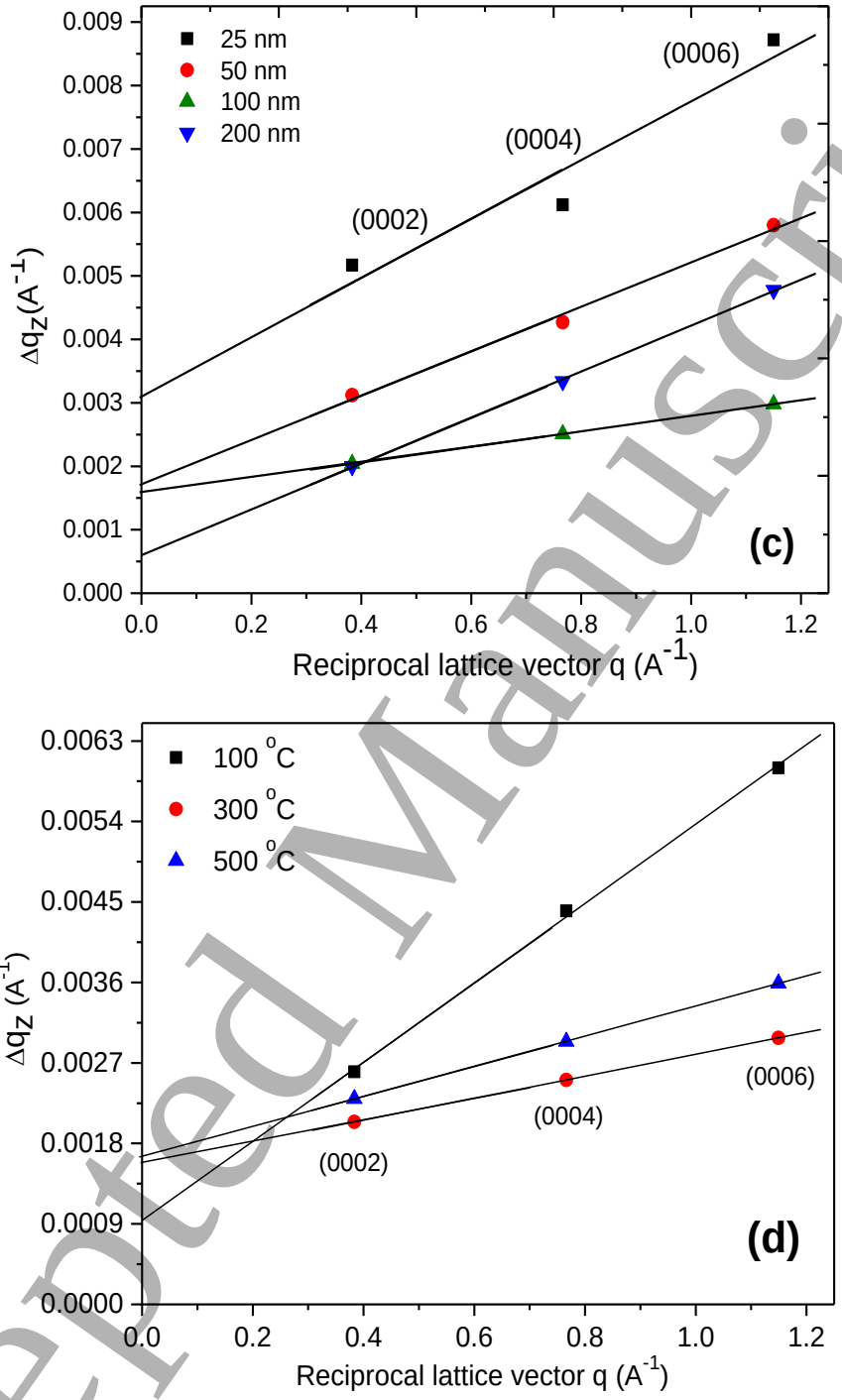

Fig 5 (a & b).